

Evaluation of High-Strength Steel Castings Possessing Improved Weldability

K. Kannan and J.J. Valencia

(Submitted 16 April 2001)

Naval components fabricated from HY-80 high-strength steels require an expensive preheat during welding to avoid heat-affected zone (HAZ) cracking. Quenched-and-tempered low-C, high-Ni steels were evaluated as potential alternatives to HY-80 steel castings with section sizes of 230 to 300 mm thickness. The investigation examined the feasibility of obtaining mechanical properties equivalent to HY-80 by heat treatment and evaluated weldability. The steel resulted in a crack-free casting, and preliminary tests suggest that it could be welded without preheating. Optimized heat treatment provided reasonably good yield strength (517 to 538 MPa) and Charpy impact toughness (63 to 80 J Charpy V-notch (CVN) energy at -73°C). The former properties were just below HY-80 casting requirements of 550 MPa. Thus, while this composition might not be a suitable replacement for HY-80, there are other potential casting applications. These include surface ship shaft struts and rudder inserts that have less stringent strength and toughness requirements.

Keywords Charpy V-notch energy, continuous cooling transformation diagrams, double tempering, hardenability, heat treatment, high-strength steel castings, HSLA-100, HY-80, Jominy test, low-carbon steels, optical microscopy, SEM and TEM characterization, Tekken test, tensile properties, welding without preheat

1. Introduction

Castings and forgings of high-strength steels, such as HY-80 and HY-100, are used on naval surface ships and submarines. Specific cast components include hull inserts, rudders, struts, stern tubes, foundations, and valve bodies. However, there are several manufacturing and fabrication problems with the castings and forgings including weldability and sensitivity to heat treatment.

The relatively high carbon and alloy content of these steels dictates a minimum preheating temperature of 107°C for sections greater than 28.6 mm thickness.^[1] This is to prevent hydrogen-assisted cracking (HAC) during welding. Furthermore, HY-80/100 castings are sensitive to heat-treatment parameters. Improper heat treatment during manufacture can result in untempered brittle martensite, which could lead to cracking even after the final tempering treatment.^[2]

Traditional high-strength steels, such as HY-80, derive their strength and low-temperature toughness from a quenched-and-tempered martensitic/bainitic microstructure. Lower carbon HSLA-80 steels typically have a ferritic microstructure, achieving their strength by precipitation hardening without significant martensitic phase transformation.^[3,4] This facilitates ease of welding, avoiding the need for a preheat. However, the HSLA-80 steel has been certified for naval applications as a replacement for HY-80 only as wrought plates^[3] and not yet as castings.

Churchill *et al.* investigated a casting with the HSLA-80 plate composition under a National Shipbuilding Research Program SP-7 project.^[4] They found that a 150 mm cubic-shaped casting exhibited poor Charpy V-notch (CVN) energies at low temperature (9 J at -73°C). The MIL-23008D specifications for HY-80 call for a minimum yield strength of 551 MPa and CVN energy of 95 J at -18°C and 68 J at -73°C .^[5] Thus, the cast HSLA-80 casting could not meet the specified minimum properties for HY-80 castings. Other studies examined castings with a composition similar to the HSLA-100 plate as a replacement for HY-80 castings with section thickness of 300 mm.^[6] However, the mechanical properties were not satisfactory (low toughness of 57 J at -73°C), though better than the cast HSLA-80 composition. Furthermore, there were noticeable macrocracks and hairline cracks, both in the as-cast and heat-treated conditions. Thus, the HSLA-100 plate composition was not found to be practical as a casting alloy for the thick sections involved.

Also in the SP-7 study, Churchill *et al.* investigated a low-C (0.04 wt.%), high-Ni (5.5%) steel with 1.5% Cr and 0.5% Mo that relied on a quench-and-temper heat treatment to achieve the combination of strength and toughness.^[4] The relatively high Ni content, in combination with Cr and Mo, was intended to limit the formation of ferrite and bainite as well as to decrease the bainite-start temperature, hence producing a finer carbide distribution within the bainitic microstructure. Both effects, in turn, were expected to improve toughness. Upon heat treatment, the casting was found to exhibit good tensile and upper-shelf CVN impact energies. However, the low-temperature (-73°C) impact properties in 300 mm thick test blocks were marginal or barely above the specified minimum for HY-80.

The present study involves investigating the potential for further optimization of alloy composition and heat treatment of alloys similar to those investigated in the preceding SP-7 study (referred to hereafter as alloys E and E-A). The objective of this work is to evaluate if modified alloy chemistries and heat treatment can lead to properties similar to the certified HY-80 composition, while being weldable with little or no preheat.

K. Kannan and J.J. Valencia, Concurrent Technologies Corporation, Johnstown, PA 15904. Contact e-mail: kannank@ctc.com.

Table 1 Chemical composition of alloys E and E-A (note higher C, Mn and La, Ce in latter)

Element	Alloy E (wt.%)	Alloy E-A (wt.%)	Element	Alloy E (wt.%)	Alloy E-A (wt.%)
C	0.032	0.061	Zr	0.006	0.01
Mn	0.91	1.1	P	0.007	0.006
Ni	5.68	5.53	S	0.0001	<0.001
Cr	1.41	1.48	Nb	0.002	0.007
Si	0.55	0.38	Ti	0.001	...
Mo	0.58	0.57	Sb	0.001	...
Ce	...	0.06	Sn	0.003	0.0078
La	...	0.02	As	0.002	...
Cu	0.16	0.11	H	1.3 ppm	...
Al	0.033	0.033	N	36 ppm	43 ppm
V	0.01	0.005

2. Technical Approach

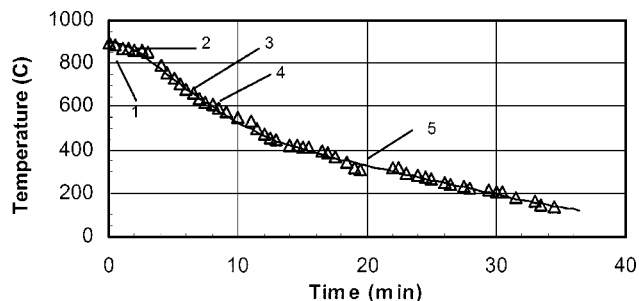
2.1 Casting Manufacturing

Castings of alloys E and E-A were procured in separate heats from a commercial steel foundry. In both cases, the steels were produced by the electric arc-furnace process and refined in an argon oxygen decarburization vessel. Alloy E was cast into a test block with dimensions $300 \times 300 \times 530$ mm. Prior to the removal of the risers and gates, the block was given a proprietary homogenization and tempering treatment. Further heat treatment (austenitization and tempering) was performed in-house on thin subsections of the casting to identify optimal heat-treatment conditions, as detailed in a later section.

Alloy E-A was melted and cast in a second heat and had a slightly modified chemistry. This composition was designed to have a somewhat higher C content (0.06%, up from 0.035%) and Mn content (1.1%, up from 0.9%) than alloy E. The higher C and Mn contents were intended to improve hardenability, which, in turn, would potentially compensate for the loss in strength upon tempering, while still ensuring weldability. Alloy E-A also had minor additions (0.06%) of rare earth metals (REM) (La and Ce) to evaluate their potential benefits in refining the as-cast microstructure and controlling the morphology of the sulfide inclusions.^[7-9] Alloy E-A was cast into blocks with dimensions of $300 \times 300 \times 530$ mm as well as $230 \times 230 \times 460$ mm to investigate the effect of section size on the mechanical properties. Unlike alloy E, these castings were fully heat treated at the foundry, adopting commercial practices. The austenitization and tempering treatments were chosen based on the best mechanical property results obtained from thin slabs of alloy E. The chemical compositions of the two alloys are provided in Table 1.

2.2 Simulated Heat Treatment of Alloy E Using Thin Slabs

A novel experimental procedure was adopted, which enabled a thin 19 mm slab to be used in each heat-treatment trial rather than the entire casting. For each heat treat and water quench operation, the cooling profile at the quarter-thickness (T/4) location of the $300 \times 300 \times 530$ mm casting was modeled by finite element methods (FEM). (The T/4 location is the location prescribed for evaluating mechanical properties in a test



1)Open Furnace 2)Remove Slab from Furnace Cover with Blanket 3)Uncover Blanket 4)Turn Fan On 5)Set Slab on Aluminum Chill

Fig. 1 Comparison of experimental cooling curves with those from FEM computations. Experimental data points are overlaid on FEM predictions (solid line)

block.^[5]) The predicted cooling rate was duplicated on the thin slab, which had been held at the desired temperature. The desired cooling rate was accomplished by using a combination of various slower cooling media, such as forced air convection, cooling in still air, wrapping the slab in an insulating blanket, *etc.* The thickness of the slab (19 mm) was decided based on considerations of the Biot Modulus, which predicted that this slab would cool uniformly with no thermal gradients for these cooling media. Further details may be obtained from Ref 6 and 10.

Figure 1 shows the calculated cooling curves overlaid with experimental results from cooling a 19 mm slab. The experimental technique affords a good match of the cooling at the desired location, while enabling considerable time and material savings and reducing experimental costs.

A potential criticism of this method is that the microstructure and chemical composition of slabs from different locations in the casting might not be representative of that at the T/4 location, notwithstanding the homogenization treatment. While that is a valid concern, the intent of these trials was merely to perform a screening of various heat-treatment operations that could be employed in heat treating a full-sized casting in a later trial. Most of the slabs used in these trials were located as close to the center of the casting as possible and between the two quarter-planes bounding the midplane. Furthermore, as will be seen in Section 4.1, Jominy end-quench tests on alloy E reveal that the hardenability behavior of samples taken from the center and from the edge of the casting are similar. This observation, along with the limited goals of this effort, precluded further consideration of the effects of segregation and inhomogeneous microstructure of the alloys studied.

2.3 Heat Treatment

Alloy E. Based on the finite element method (FEM) simulations, the heat-treatment evaluation of alloy E was conducted on slabs of a 300×300 mm section and 19 mm thickness. Table 2 shows the heat-treatment range employed. The austenitizing and tempering temperature ranges were chosen from the literature,^[4] and the hold time at temperature was chosen following typical industrial practice for heavy-section steel castings and forgings (1 h for up to 25 mm in thickness, plus 30 min for each additional 25 mm).^[11] Some sections of alloy E

received a double-tempering treatment, as in the SP-7 study,^[4] while others received only a single temper.

Alloy E-A. The knowledge gained regarding the effect of various heat treatments on the mechanical properties was then used to select the optimum heat treatment for the full-sized castings of alloy E-A. This is shown in Table 3.

2.4 Mechanical Properties and Microstructure Evaluation

Tensile and CVN impact properties were evaluated according to ASTM Standards E-8 and E-23, respectively.^[12,13] These were evaluated on the heat-treated slabs of alloy E and at the T/4 location for alloy E-A. The tensile results reported are the average of two tests on standard 13 mm gauge diameter samples conducted at 25 °C, while the CVN results represent the average of 5 tests on standard 10 mm square cross-section samples, conducted at -18 and -73 °C. Limited dynamic tear (DT) testing^[14] was also performed to determine the DT energies at -40 °C. Metallographic samples taken from the tensile and CVN specimens representing various heat-treatment conditions were evaluated by optical microscopy. Limited transmission electron microscopy (TEM) was used to examine double-tempered structures from alloy E, and x-ray diffraction was employed to determine retained austenite. Scanning electron microscopy (SEM) was used to inspect the tensile and CVN fracture surfaces.

2.5 Weldability

Weldability of alloy E was evaluated by the Tekken test that has been standardized by the American Welding Society (AWS B4.0-95).^[15] Here, a single test weld is deposited on the sample of the appropriate “Y-groove” configuration. Weldments are then inspected for signs of HAC, either in the weld metal (WM) or HAZ. Welding was done under controlled conditions of 16 °C (*i.e.*, no preheat) and 82% relative humidity to simulate shipyard welding on a cold, humid day. Welding was performed under the following conditions:

- shielded metal arc welding (SMAW) using E-10018M electrode, 1.1 kJ/mm energy input, and
- gas metal arc welding (GMAW) using MIL-100S electrode and an experimental lower carbon LC-100 electrode with 1.46 kJ/mm energy input.

Alloy E was compared to various traditional steels (an HY-80 equivalent A757-EQ21 casting and an HY-100 plate).

3. Results

3.1 Alloy E Casting

Tensile and CVN Impact Properties. The tensile and CVN impact properties of alloy E were evaluated over a wide range of austenitization, tempering, and double tempering temperatures. In general, it was found that the austenitizing temperature did not have a significant effect on the tensile properties over the temperature range of 899 to 954 °C. For example, in the single-tempered condition (677 °C), the same yield strength of 607 MPa was obtained in samples austenitized at 899 °C as well as 954 °C. The Charpy values also appeared comparable within the range of scatter (51 ± 25 J and 48 ± 13 J at -73 °C after austenitizing at temperatures of 899 and 954 °C, respectively, and tempering at 677 °C). It was also found that a single subcritical temper (*i.e.*, below $A_{c1} = 665$ °C^[16]) was not sufficient to produce the desired combination of yield strength and low-temperature toughness. It appeared that a double-tempering operation consisting of an intercritical temper followed by a subcritical temper was required to improve low temperature toughness.

Table 4 shows the best tensile and CVN properties of alloy E resulting from single intercritical-tempering treatments and those resulting from a double-tempering treatment (intercritical followed by subcritical) at the temperatures indicated. The CVN energy values are shown along with the 95% confidence limits.

Following austenitization and a single temper in the 677 to 705 °C range, alloy E exhibited adequate tensile properties and upper-shelf CVN energies at -18 °C, sufficient to meet MIL-S-23008D requirements for HY-80. However, the CVN properties at -73 °C were not achieved. The double-tempering treatment at 621 °C increased CVN impact properties at both temperatures as well as the DT energy, but the yield strength values were reduced to below the 551 MPa minimum specified for HY-80. Thus, though this heat treatment leads to satisfactory impact properties, it did not meet MIL-S-23008D strength requirements. The best combination of strength and toughness was obtained upon an intercritical temper in the 677 to 705 °C range, followed by a subcritical temper at 621 °C.

Table 2 Temperature range used in heat treatment of alloy E

Austenitization	First temper	Second temper
899 to 954 °C Water quenched(a)	649 to 732 °C Water quenched(a)	<ul style="list-style-type: none"> • None • 566 to 621 °C water quenched(a)

(a) Cooling rate equivalent to water quench for a 300 mm thick casting, calculated from the FEM model

Table 3 Heat treatment of full-sized blocks of alloy E-A

Composition/ Block ID	Dimensions (mm)	Preliminary HT	Austenitization	Temper	Second temper
E-A-1	300 × 300 × 530	Proprietary homogenization and appropriate temper for removal of gates and risers	927 °C/6.5 h water quench	691 °C/6.5 h water quench	621 °C/2 h water quench
E-A-2	230 × 230 × 460		927 °C/5 h water quench	691 °C/5 h water quench	621 °C/2 h water quench

Table 4 Optimum mechanical properties of alloy E

Austenitization (°C)	First temper (°C)	Second temper (°C)	Tensile properties (room temperature)				CVN energy (J) and % shear		DT energy (J) and % shear
			Yield strength (MPa)	Tensile strength (MPa)	Elong. % 51 mm gauge	Reduction in area (RA),%	-18 °C	-73 °C	-40 °C
927	677	None	607	869	24	71	133 ± 24 100%	61 ± 9 28%	805 67%
		621 (2 h)	538	724	27	72	195 ± 11 100%	92 ± 24 44%	1205 100%
	705	None	690	959	18	65	121 ± 8 100%	49 ± 9 47%	418 43%
621 (2 h)		531	745	26	71	193 ± 11 100%	91 ± 30 49%	1159 100%	
HY-80 MIL-S-23008D specifications (minimum)			551	...	20	...	95	68	...

Microstructure and Fracture Evaluation. Microstructural examination of the homogenized cast material revealed the presence of a very coarse microstructure with a prior-austenite grain size ranging from 250 to 300 μm. The coarse microstructure may be expected due to the large size of the casting. The microstructure also consisted of lath ferrite, surrounding small regions of angular/blocky bcc phase, with small amounts of retained austenite (1 to 3%).

The prior-austenite grain size of the austenitized, single- and double-tempered material was found to have a considerable scatter. For example, samples from single tempered material at 677 °C/1 h after austenitization at 927 °C/1 h varied from 27 to 65 μm. Double-tempered samples at 677 °C/6.5 h and 593 °C/6.5 h after austenitizing at 927 °C/6.5 h showed a grain-size range of 21 to 60 μm. Thus, a direct correlation between the heat treatment and grain size was not possible. However, the heat treatments used substantially refined the microstructure of the initial homogenized cast material.

Figure 2 shows the light optical microstructures (LOMs) of alloy E in the single- and double-tempered conditions, respectively. Note that single- and double-tempered materials did not reveal clear differences in their microstructure, which primarily consisted of bainite, some ferrite, and possibly some martensite, as shown in Fig. 2(b) and (d), respectively. Additionally, independent of the heat treatment employed, the “dendrite ghosts” of the as-cast microstructure are still reminiscent (Fig. 2(a) and (c)). Further TEM inspection of the double-tempered specimens by Fonda *et al.*^[17] indicated that the microstructure primarily consisted of ferrite laths, a highly dislocated lenticularlike bcc phase, and very small amounts of retained austenite (Fig. 3). X-ray diffraction of the double-tempered steel indicated retained austenite levels of approximately 0.3%.

As a note of reference, the microstructures following similar double-tempering treatments were examined earlier.^[4,18] It has been suggested that the improvement in toughness following a double temper is due to the following. During the first (inter-critical) temper, some of the existing microstructure transforms to austenite while the rest undergoes overtempering (softening). Upon water quenching, the austenite transforms to martensite. In the second (subcritical) tempering operation, the martensite is tempered, thus leading to overall improved toughness.

In general, inspection of the CVN fracture surfaces revealed that all samples tested at -18 °C exhibited a fully ductile behavior (Fig. 4a). Conversely, both single- and double-tempered samples tested at -73 °C had a mixture of ductile and

brittle fracture (Fig. 4b and 5a and b), with the double-tempered samples exhibiting more ductile behavior than the single-tempered samples (Fig. 4b versus 5b). It was also observed that samples with a smaller and narrower prior-austenite grain-size range, in both single- and double-tempered conditions, had a higher CVN energy than those with a larger size distribution. For example, a CVN energy of 75 J was obtained from a double-tempered material (677 °C/6.5 h and 593 °C/6.5 h after austenitizing at 927 °C/6.5 h) with a prior-austenite grain size of 24 to 34 μm. Specimens with the same tempering conditions and a prior-austenite grain size of 21 to 52 μm had a CVN energy of only 48 J. An additional feature of many fracture surfaces was the presence of relatively large inclusions (5 to 15 μm). Energy dispersion spectroscopy (EDS) analysis indicated that the inclusions were complex oxides containing primarily Al, Ca, Fe, Ni, and Zr (Fig. 5c). Their presence may have adversely affected the impact energies and other mechanical properties.

Weldability Evaluation of Alloy E. Tekken tests using SMAW of alloy E and HY-100 using E10018-M revealed significant differences (Fig. 6a and b). HY-100 exhibited poor weldability with HAZ and WM cracking. This is as expected for a higher carbon steel welded without preheat. On the other hand, alloy E exhibited no HAZ cracks, indicative of better weldability. However, it had WM cracks, indicating the need for a more “hydrogen-free” process such as GMAW with different consumables, for instance, MIL-100S or the lower carbon LC-100. While the MIL-100S electrode is sometimes used for welding thin sections without preheat, in the present case, it resulted in WM cracks and some HAZ cracks (not shown) and, thus, was not found to be suitable. Figure 6(c) shows the weldment of alloy E obtained by GMAW using the experimental electrode, LC-100, which was formulated to be used without preheat. This exhibits good weldability, as seen by the absence of cracks either in the WM or HAZ. However, due to material limitations, only one valid test was performed for alloy E under this condition, while the AWS-4.0 test procedures call for a minimum of three. Thus, the tests were not conclusive, but preliminary results were encouraging.

3.2 Alloy E-A Castings

Tensile and CVN Impact Properties. The tensile and CVN impact properties of castings E-A-1 and E-A-2, evaluated at the T/4 location, are listed in Table 5.

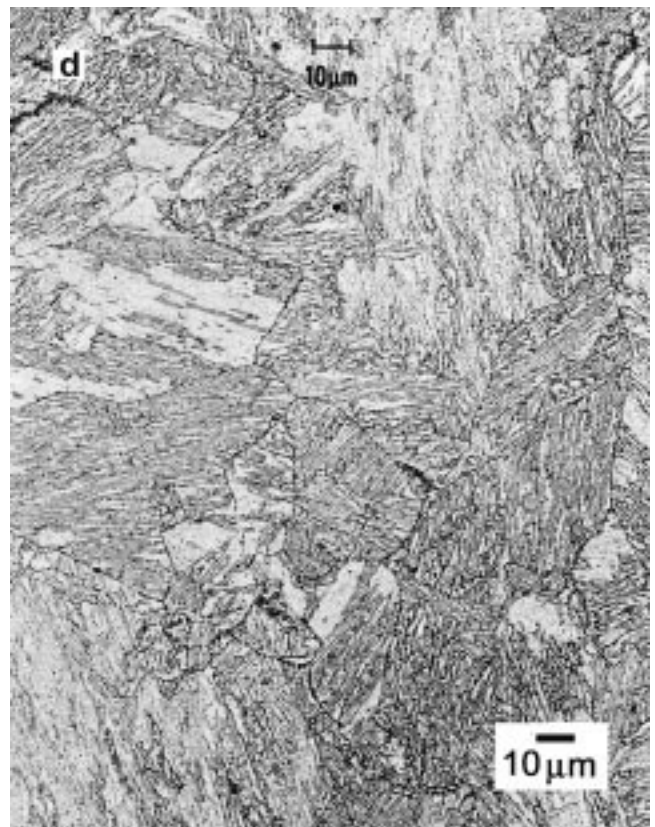
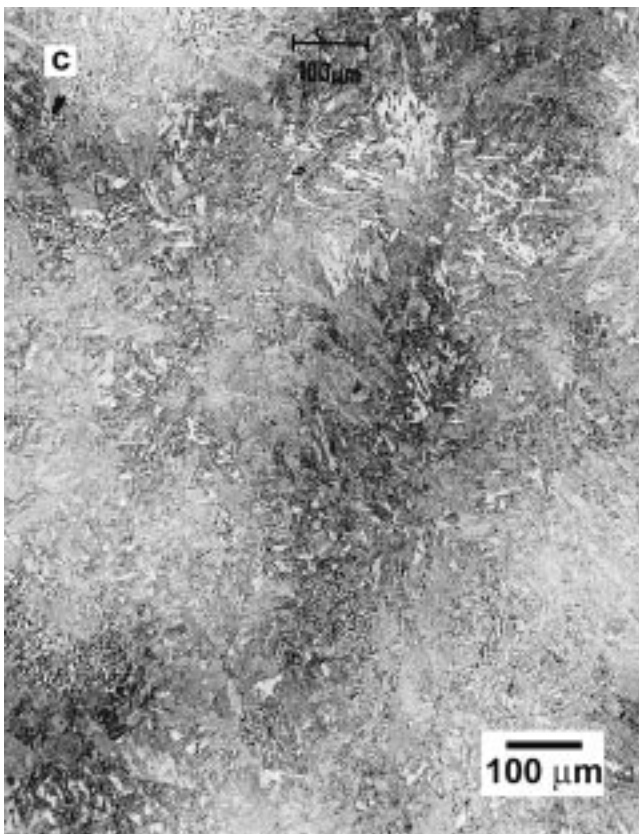
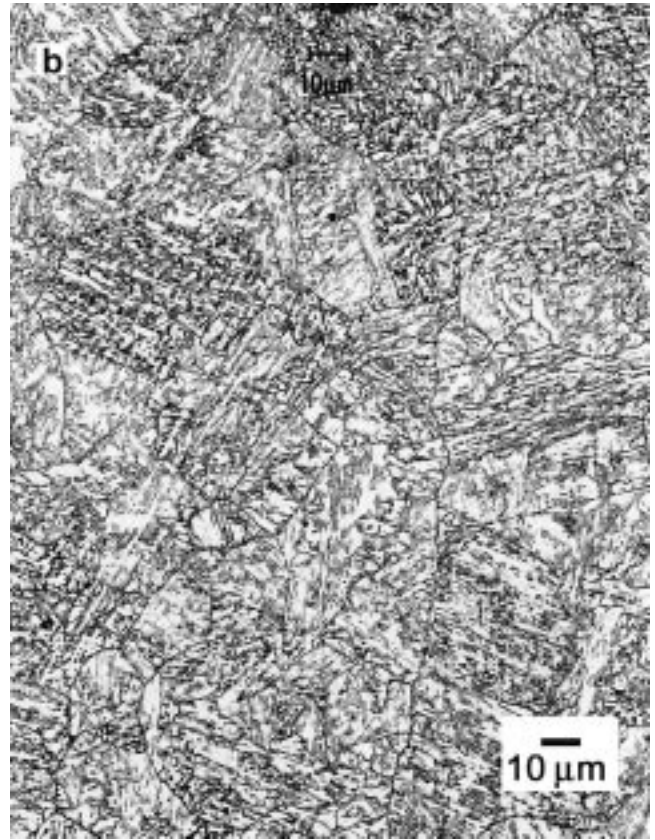
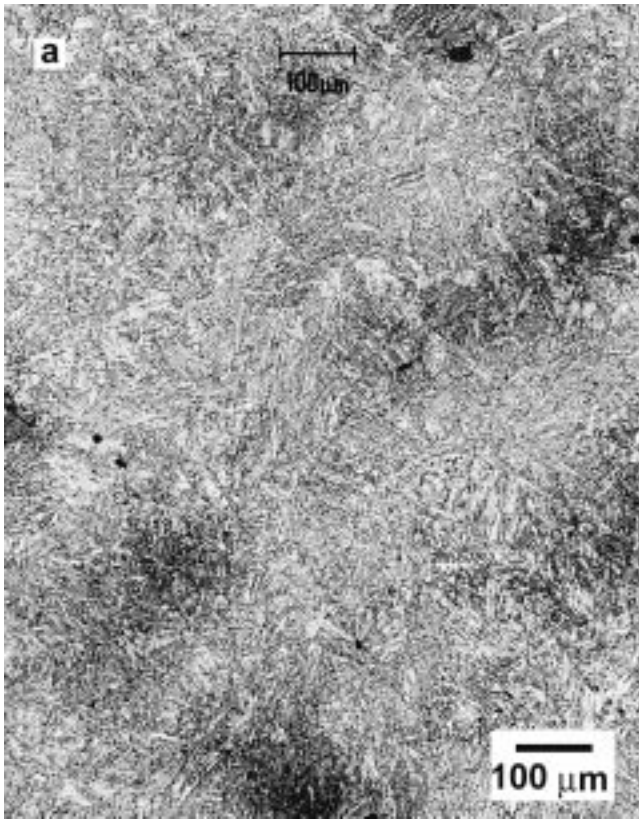


Fig. 2 Optical microstructures of alloy E austenitized at 927 °C/6.5 h: (a) and (b) single tempered at 677 °C/1 h, and (c) and (d) double tempered at 677 °C/6.5 h + 593 °C/6.5 h. Etchant: modified Winsteads and 2% Nital

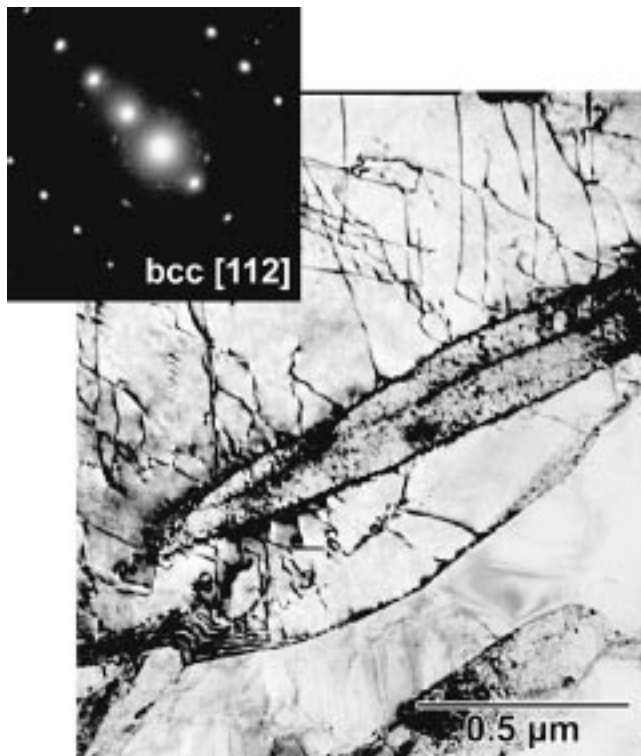


Fig. 3 The TEM microstructure of double-tempered E-steel showing mostly lath ferrite, some bcc-ferrite, and possibly small pockets of austenite

Note that yield-strength values are in the range of 517 to 538 MPa and, thus, fall short of HY-80 requirements. These may be compared to the results in Table 4, based on subscale heat treatment of alloy E. The austenitization and tempering treatments in both cases (alloy E subscale and alloy E-A full scale) were quite similar. It may be seen that the yield-strength values are in the same range (531 to 538 MPa for E and 517 to 538 MPa for E-A). At first glance, it would appear that the alloy modifications (such as increased C and Mn) did not lead to any significant improvement in hardenability, at least for the section sizes under consideration.

The elongation at failure and reduction in area are quite low, indicative of hydrogen embrittlement (HE) problems. Interestingly, HE problems were not encountered in the trials done on alloy E castings, where heat treatment was performed on 19 mm slabs cut from the castings. This appears to be a potential problem in heat treatment of thick sections. It is likely that there is considerable microshrinkage and porosity at the midplane of such a thick section, where hydrogen would tend to accumulate. If this is not diffused out or dispersed by a hydrogen-baking treatment, HE is a strong possibility. An experimental baking treatment of 232 °C/24 h was tried on tensile samples machined from regions adjacent to the T/4 location. This increased the elongation to failure to 25%, while the yield strength was unaffected. Thus, this seemed to be an appropriate treatment for eliminating HE, at least for the thin sections employed (13 to 19 mm thick). Thicker sections might call for increased temperature and/or holding time.

Analysis of the yield-strength values in conjunction with

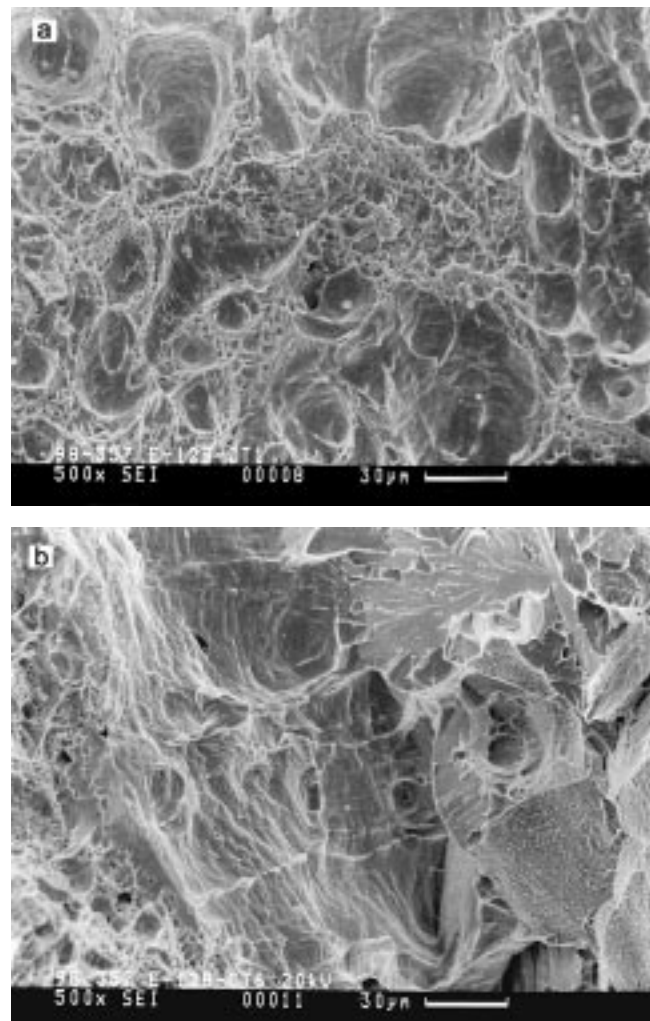


Fig. 4 The SEM image of fractured Charpy samples of alloy E (double tempered): (a) tested at $-18\text{ }^{\circ}\text{C}$ and (b) tested at $-73\text{ }^{\circ}\text{C}$

the CVN energies indicates that the desired combination of these properties has not been achieved. Satisfactory CVN energies, as seen in the case of E-A-2, appear to be combined with relatively low yield strengths. Another feature of the impact testing was the nature of fracture surfaces observed. Several samples exhibited an anomalous appearance, marked by the presence of “flat facets,” in addition to the usual ductile dimples or trans- and intergranular cleavage. This has been referred to in the past as “rock candy fracture” (RCF).^[19] The reasons behind RCF are not quite clear; it has been previously speculated that aluminum nitride (AlN) embrittlement might be a probable cause.^[19] While RCF can lead to lower CVN energies, another effect of RCF is to increase the scatter in CVN energy data.

While the mechanical properties obtained from these full-sized castings fall short of HY-80 specifications, they represent an improvement over results from prior investigations.^[4,6] These castings possess improved low-temperature ($-73\text{ }^{\circ}\text{C}$) impact properties than cast HSLA-80 and HSLA-100 blocks (Table 6). These castings could also be cast and heat treated without any cracking problems, as encountered with the HSLA-100 composition.

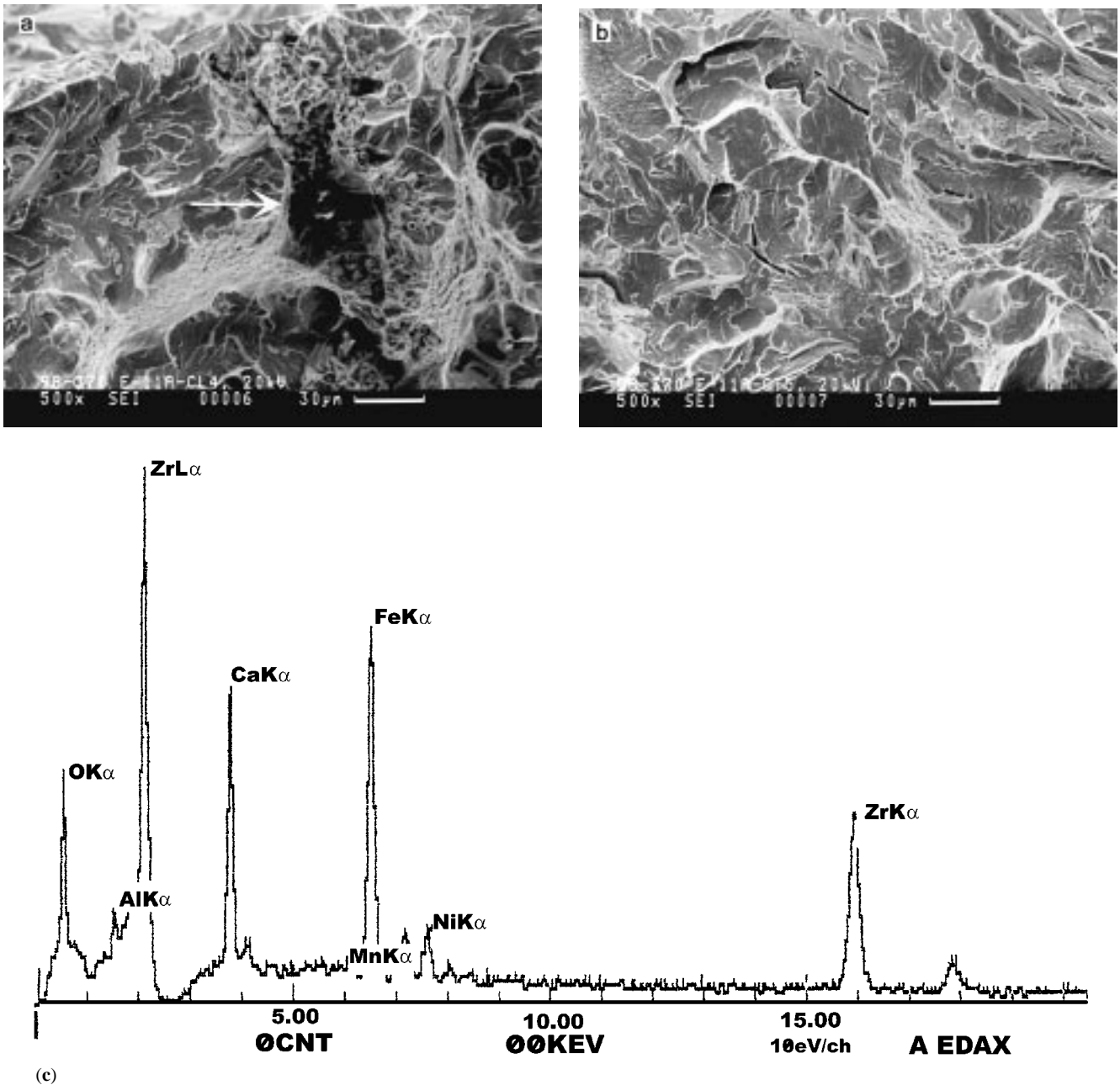


Fig. 5 The SEM image of fractured Charpy samples of alloy E (single tempered) (a) tested at $-73\text{ }^{\circ}\text{C}$, (b) tested at $-73\text{ }^{\circ}\text{C}$, and (c) EDS spectra of inclusion shown by the arrow in (a)

Microstructure Evaluation. Optical microscopic examination of E-A steel castings showed that the microsegregation of the as-cast material persisted even after homogenization and full heat treatment. Figure 7 shows the macrostructures found in CVN specimens taken from the 230 mm thick casting.

In general, these castings had a greater extent of microsegregation and a higher porosity level than the castings of alloy E. The dendrite arm spacing, which is an indicative parameter of microsegregation, was found to be $\sim 400\text{ }\mu\text{m}$ in E-A compared to 170 to $240\text{ }\mu\text{m}$ in alloy E. The reasons for this are unclear; the modified alloy chemistry or a change in the melting and pouring process may have contributed to some degree.

Most of the porosity was found at the dendrite ghosts of the interdendritic regions of the castings, as shown in Fig. 7. In addition to shrinkage porosity, other regions of the specimens showed porosity with rounded features, which may be indicative of gas porosity. An example is shown in Fig. 8.

The SEM examination (Fig. 9) also revealed the presence of relatively large clusters of REM inclusions ($>10\text{ }\mu\text{m}$). The EDS spectrum (Fig. 9b) of the REM oxide inclusions in alloy E-A also indicates the presence of sulfur and some aluminum. The REM inclusions tended to be associated with porosity.

The LOM analysis indicated that the microstructure of the steels in the fully heat-treated condition consisted primarily

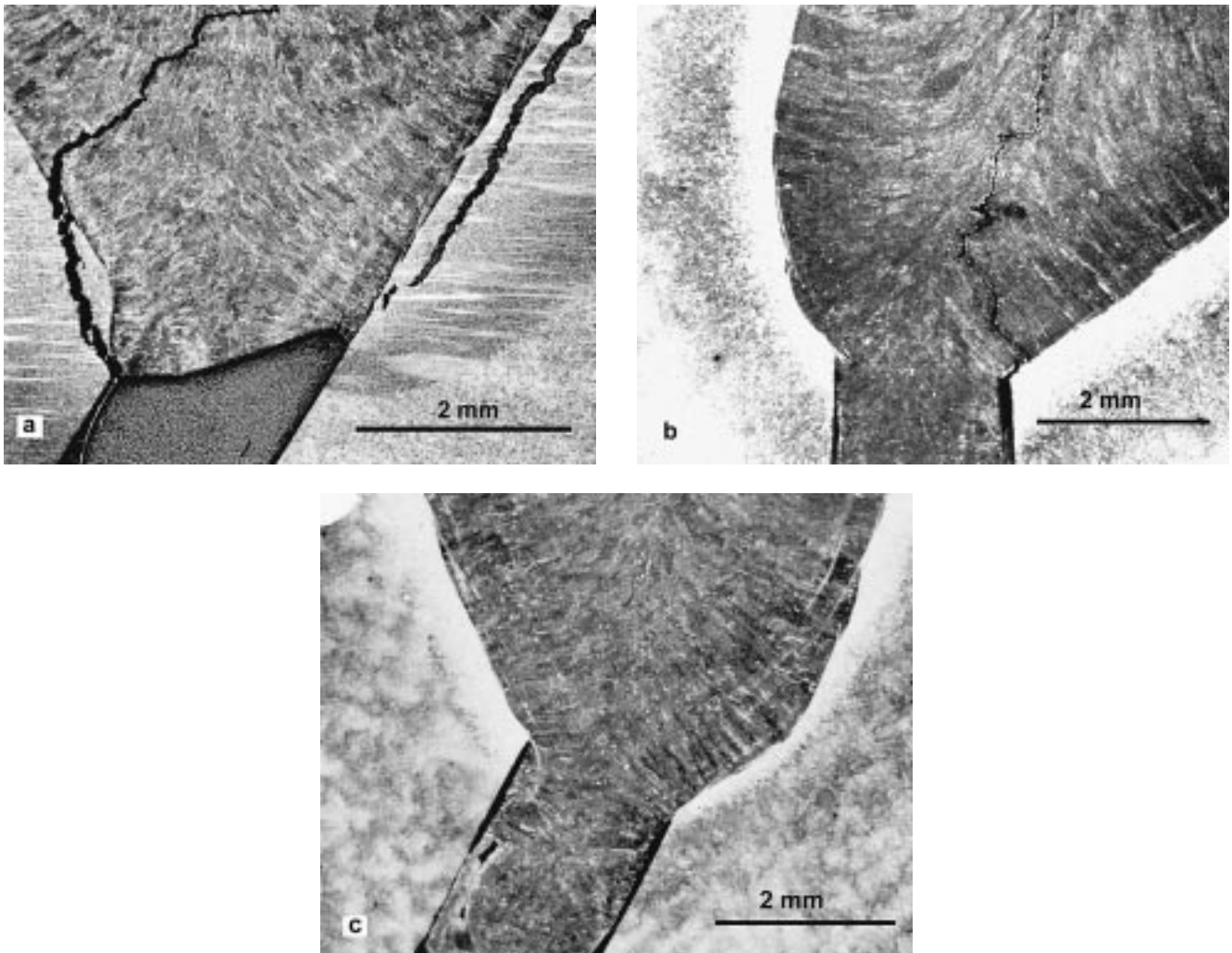


Fig. 6 Low magnification pictures of Tekken test weldments: (a) HY-100, SMAW (MIL-10018); (b) alloy E, SMAW (MIL-10018); and (c) alloy E, GMAW (LC-100). All tests performed at 16 °C, 82% relative humidity, 1.1 to 1.46 kJ/mm energy input

Table 5 Mechanical properties of E-A-1 and E-A-2 castings at T/4 location

Alloy	Section size/ block ID	Tensile properties (room temperature)				CVN energy (J) and % shear		Comments
		YS (MPa)	TS (MPa)	Elong. % 51 mm gauge	RA, %	-18 °C	-73 °C	
E-A	300 mm (E-A-1)	538	662	7	20	99 ± 34 35%	79 ± 31 35%	HE in all tensiles(a)
	230 mm (E-A-2)	517	717	11	22	123 ± 22 50%	80 ± 26 36%	HE in all tensiles
MIL-S-23008D specifications (minimum)		551	...	20	...	95	68	...

(a) HE = hydrogen embrittlement

of bainite with some ferrite and possibly very small pockets of martensite (Fig. 10).

Also, no differences in microstructure (at the LOM level) were found between the interdendritic and dendrite areas in this steel, except that the prior-austenite grain size at the interdendritic regions appeared to be 30 to 40% smaller than at the

dendrite regions. However, the variations observed in prior-austenite grain size may be attributed to the large variations in cooling rates from the surface to the center of the casting from solidification to temperatures below A_{c1} .

Table 7 shows the prior-austenite grain-size ranges for samples from heat-treated alloys E-A and alloy E. Note that

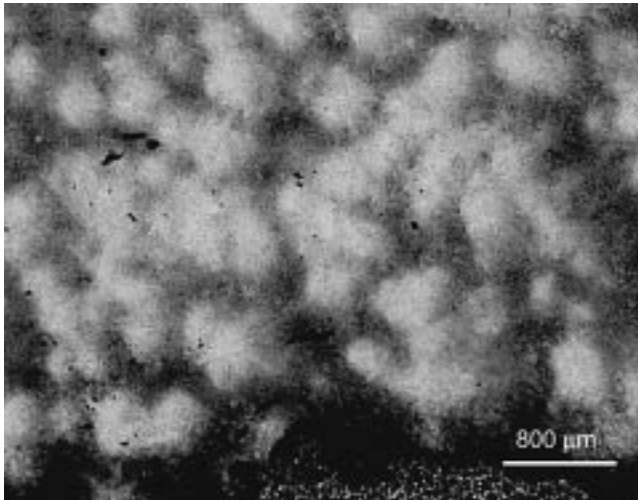


Fig. 7 Low magnification optical microstructures of homogenized and heat-treated (Table 3) 230 mm section thickness steel E-A

Table 6 Mechanical properties of HSLA-80 and HSLA-100 castings from literature

Casting composition	Section size (mm)	Tensile properties (room temperature)		CVN energy (J)	
		YS (MPa)	TS (MPa)	CVN energy (J)	
				-18 °C	-73 °C
HSLA-80 ^[4]	150	546	625	130	9
HSLA-100 ^[6]	300	558	703	138	57

the grain size for commercial HY-80 steel is given for comparison.

While there is a large variation in the prior-austenite grain size within and among the various castings, it would appear that E-A castings have a narrower and relatively smaller prior-austenite grain-size range than alloy E. However, both alloy E and E-A steels have a coarser prior-austenitic structure than the HY-80 steel, despite the latter having a larger cross section (note that different vendors manufactured HY-80 and E-steels).

Large variations in prior-austenite grain size may be expected in castings with large cross sections. These variations may be attributed to the chemical composition, manufacturing practices that vary from vendor to vendor (melting, deoxidation, alloying, pouring parameters, casting size, mold materials, design, *etc.*), and homogenization treatment. The difference in parameters, such as dendrite arm spacing and porosity, between the two batches of castings also indicates that the casting process was not standardized (especially for these experimental alloys). More work is needed to determine the effects of casting manufacturing parameters and solidification phenomena (microsegregation and solidification rates within the casting) on the parent-austenite grain size. This would help develop techniques to control the grain size for the optimization of microstructure and mechanical properties.

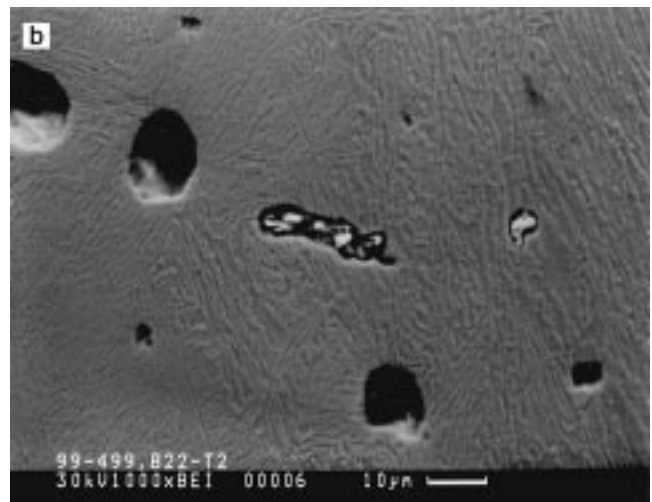
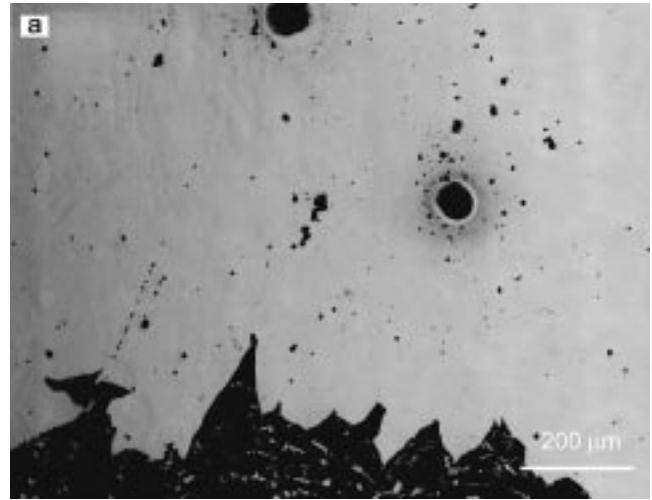


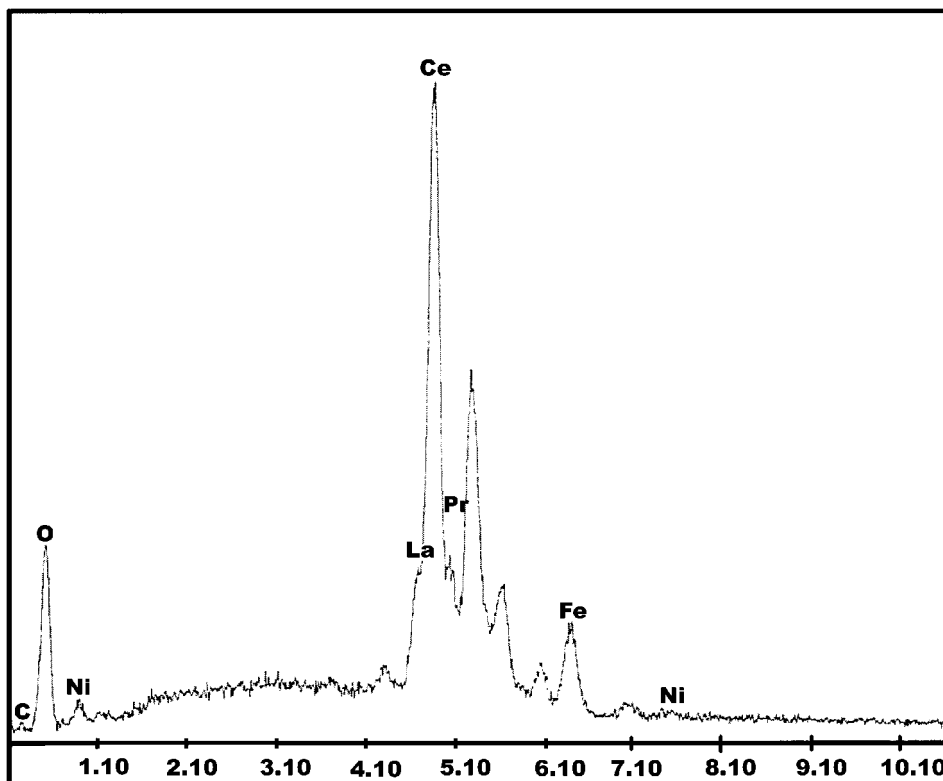
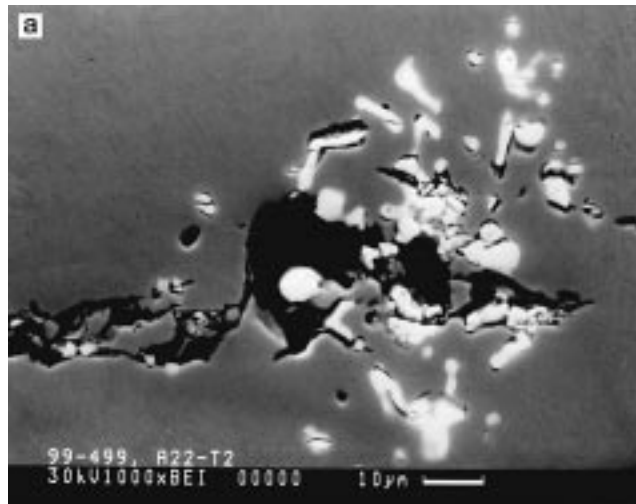
Fig. 8 Porosity in homogenized and heat-treated (Table 3) 230 mm section thickness casting of alloy E-A: (a) light optical view and (b) SEM view

4. Discussion

The quenched-and-tempered low-C, high-Ni steel compositions (alloy E and its modification E-A) resulted in crack-free castings. Preliminary tests suggest that alloy E can be welded without preheat. However, neither E nor E-A achieved the required mechanical properties to meet MIL-S-23008D for HY-80 castings. This is perhaps indicative of a lack of hardenability or a nonoptimal microstructure of the alloys studied. To address these issues, the hardenability of these steels was evaluated using the Jominy test,^[20] in conjunction with relevant continuous cooling transformation (CCT) diagrams. Second, the casting results were compared with mechanical property data from forgings, which were made from a casting of the same alloy E.^[21]

4.1 Hardenability

A potential factor in the relatively low mechanical properties of these steel castings is their hardenability. This can be seen



(b)

Fig. 9 The SEM views and EDS spectra of REM inclusions in alloy E-A

from Fig. 11, which compares the hardenability for alloy E and the HY-80 equivalent steel (A757 E2Q1 steel cast as a $350 \times 350 \times 1050$ mm block). Note that the data presented in Fig. 11 are from samples taken from the center as well as closer to the surface of the castings, in order to account for potential effects of segregation. The HY-80 steel exhibits a hardness of about 41 R_C (Rockwell C) at the quenched end, similar to what might be expected of a martensitic structure for that carbon content.^[22] With increasing distance from the quenched end (*i.e.*, with decreasing cooling rate), there is a gradual decrease

in hardness to about 39 R_C. On the other hand, alloy E exhibits a considerably lower hardness than HY-80, and the hardness throughout the sample remains practically constant (32 to 33 R_C). The lack of a significant hardness variation with distance indicates that alloy E is insensitive to cooling rates. It is also interesting to note that the hardness of the samples taken from the center and those taken closer to the surface of the casting are quite similar. Thus, segregation, if present, does not appear to have a significant effect on the hardenability in both steels.

This relative insensitivity of hardness to cooling rate was

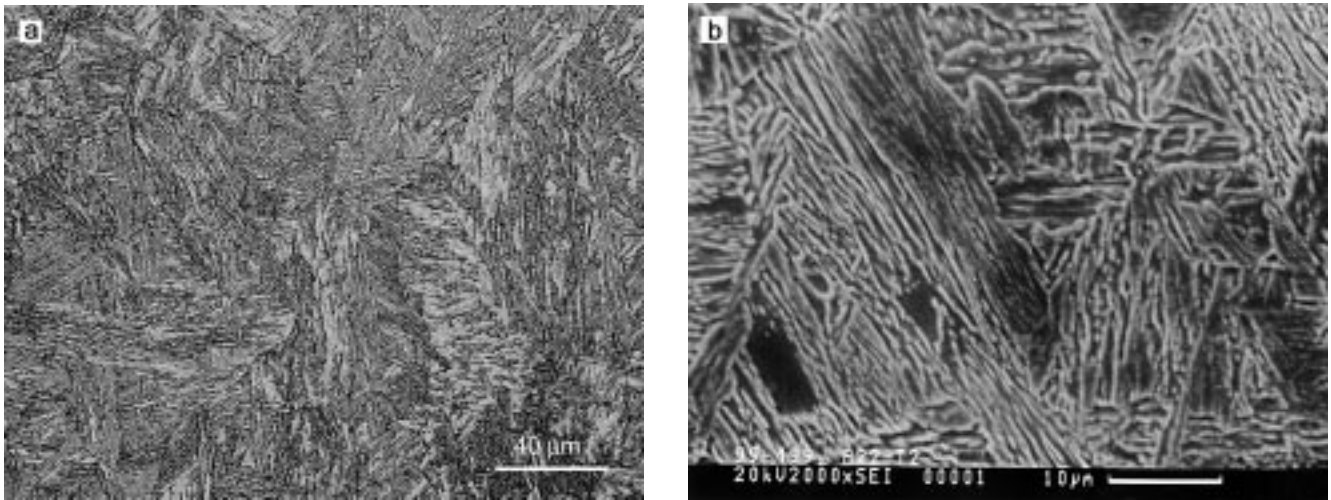


Fig. 10 Optical and SEM microstructures of fully heat-treated alloy E-A casting

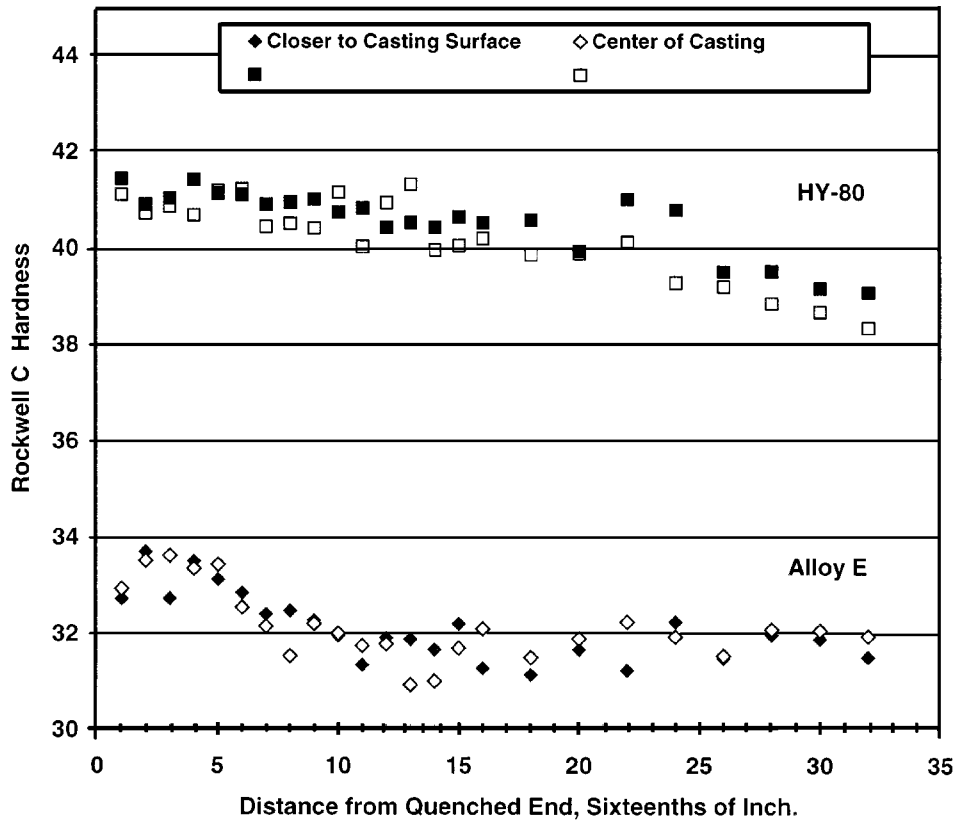


Fig. 11 Jominy hardenability for alloy E and HY-80 equivalent (A757 E2Q1) cast steels austenitized at 927 °C and 899 to 921 °C for 1 h per squared inch, respectively

Table 7 Prior-austenite grain size in alloys E-A, alloy E, and HY-80 steel

	Alloy E-A-2		Alloy E	HY-80 casting
Casting section, mm	230 × 230 × 460	300 × 300 × 530	300 × 300 × 530	990 × 990 × 330
Grain size range, μm	27–35	32–45	21–60	~16
ASTM	7.2–6.7	7–6	8–4.7	9

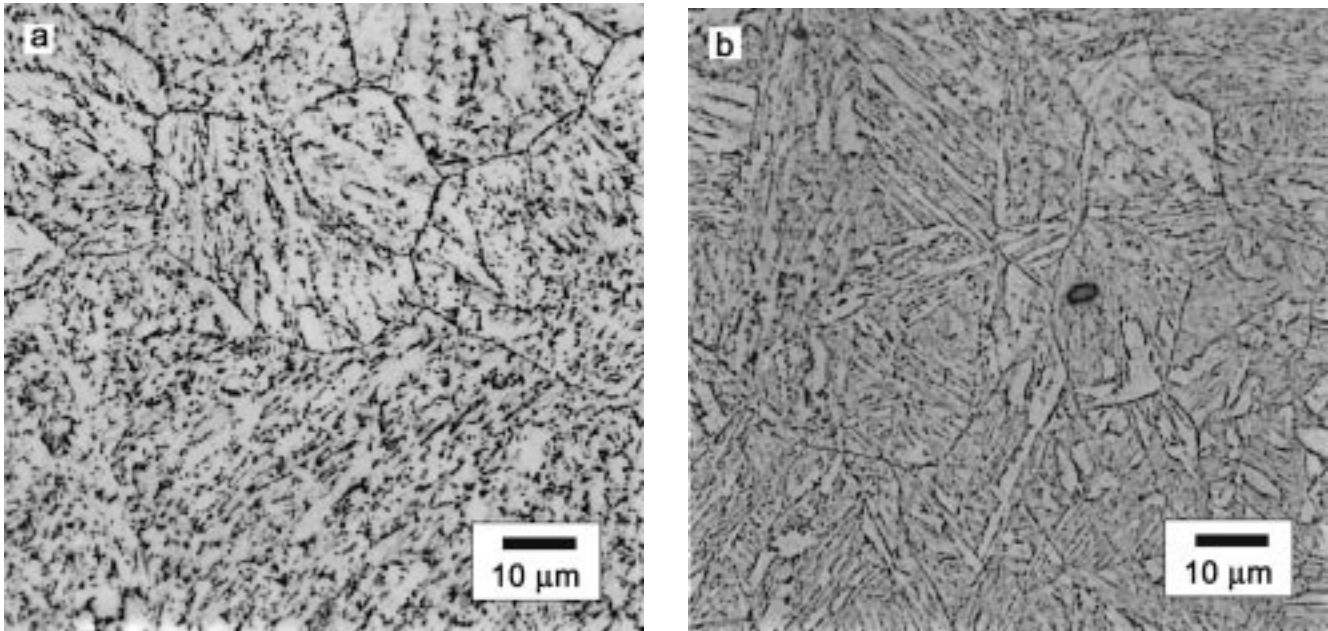


Fig. 12 Optical microstructures and hardness values of samples of alloy E-A that were controlled cooled from approximately 1000 °C: (a) cooled at 0.5 °C/min, 332 HV and (b) cooled at 132 °C/min, 343HV. Etchant: modified Winsteds and 2% Nital

observed in alloy E-A castings as well. This was evident from a microstructural and hardness analysis of samples subjected to controlled fast and slow cooling cycles, as shown in Fig. 12. The microstructure of the sample cooled at 132 °C/min was found to be predominantly martensitic with a hardness of 343 HV ($\sim 35 R_C$), while that of the slow-cooled sample (0.5 °C/min) was mostly bainitic with a hardness of 332 HV ($\sim 33 R_C$). Thus, the hardness of martensite is fairly similar to that of bainite, perhaps due to the low carbon content of the martensite produced and with the resultant body-centered tetragonal (bct) structure having a low c/a ratio. The insensitivity to cooling rate is also in keeping with the properties of the 300 and 230 mm thick castings of Table 5. This analysis shows that the maximum hardness values of alloy E (from the Jominy test) and alloy E-A (from the controlled cooled sample) are quite similar, indicating that the slight increases in C and Mn in the latter had no effect on promoting hardening.

The lack of hardenability may be further corroborated by an inspection of a partial CCT diagram developed for alloy E-A^[6] and overlapped with that of a similar alloy (1118) from the SP-7 study.^[4] This is shown in Fig. 13, along with the predicted cooling rate at the T/4 location for a 125 mm and a 300 mm thick section subjected to water quench. The 300 mm thick section results in a nonmartensitic structure upon austenitization and quench from 927 °C. This correlates well with the bainitic microstructure observed in this alloy (Fig. 10).

Quantitative estimates of hardenability, such as the ideal critical diameter (D_I), have been established mostly for medium-carbon steels.^[22] The D_I is a measure of the thickest round bar of a given composition that will result in at least 50% martensite at its center, given a perfect quench. Such data are not available for lower carbon alloys, such as alloy E. To a first approximation, a section size of 125 mm or less might produce a significant amount of martensite, as shown in Fig. 13. However, even if a

predominantly martensitic structure were obtained, the hardness would not be comparable to that of HY-80. Note that the E-A sample cooled at 132 °C/min gave a hardness of 35 R_C (343 HV), which is lower than the hardness of 41 R_C at the water-quenched end of HY-80. This is primarily due to the low carbon content in alloy E.

4.2 Comparison of Casting and Forging Properties

Analysis of tensile and CVN impact properties of alloy E in the forged condition^[21] showed that the specified properties in alloy E could be achieved by refining the microstructure and closing porosity by forging. In this case, the forged and fully heat-treated material had a prior-austenite grain size of approximately 18 μm (8.4 ASTM) with a primarily bainitic microstructure. The results are compared in Table 8.

This analysis indicates that it would be very difficult for alloy E to meet the MIL-S-23008D specified mechanical properties in the cast form. However, microstructural refinement and elimination of casting defects, such as porosity, may result in better and more consistent properties than those observed in the castings of this investigation.

5. Conclusions

Quenched-and-tempered low-C, high-Ni steels were evaluated as potential alternatives to HY-80 castings. The focus of the study was on optimizing the heat treatment to obtain mechanical properties equivalent to HY-80 and evaluating their weldability. The results of this study indicate that the compositions studied were not completely able to meet the tensile and CVN impact properties specified by MIL-S-23008D for HY-80 cast steels. However, significant improvements in the heat

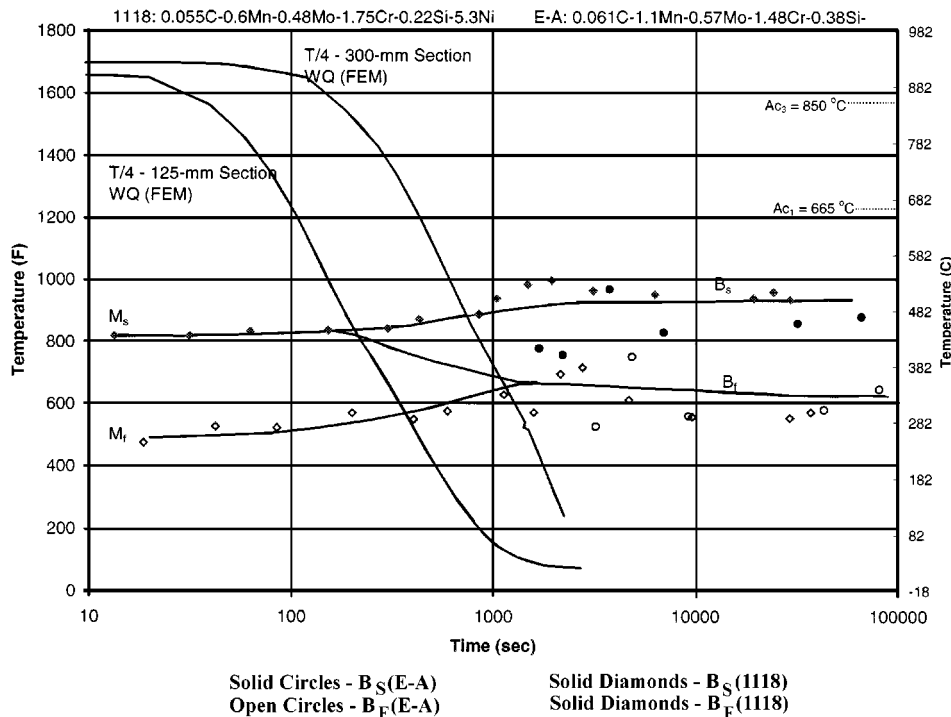


Fig. 13 The CCT diagrams for alloy E-A and alloy-1118 from Ref 4

Table 8 YS and CVN properties for alloy E forged at 1093 °C

Normalizing/ austenitizing (°C)	Tempering (°C)	YS _(0.2%) L/T (MPa)	CVN at -18 °C/-84 °C (J)	Reduction ratio
1010/927	649	594/598	206/133	3:1
1010/927	649	566/571	197/119	5:1

treatment of the low-C, high-Ni steels were achieved. A double-tempering treatment led to reasonable yield strength (517 to 538 MPa) and CVN energy (80 J at -73 °C) in castings with 230 to 300 mm thick sections. This represents a considerable improvement over the cast HSLA-80 and cast HSLA-100 compositions, especially with regard to low-temperature CVN impact properties. The castings of the alloys studied were reasonably sound and free of cracks, and preliminary tests suggest that castings of this material could be welded without preheat. Thus, while this alloy cannot be a direct replacement for cast HY-80, there might be other potential applications for which this could be considered. These include surface ship shaft struts and rudder inserts with less stringent strength and toughness requirements.

Acknowledgments

This work was conducted by the National Center for Excellence in Metalworking Technology, operated by Concurrent Technologies Corporation under Contract No. N00014-00-C-0544 to the U.S. Navy as part of the U.S. Navy Manufacturing Technology Program. The authors acknowledge the technical contributions and advice of Paul Konkol and Gerard Mercier, Concurrent Technologies Corporation, and Dr. Richard Fonda,

Naval Research Laboratory, in performing TEM characterization of the alloys.

References

- Anon.: "Fabrication, Welding and Inspection of HY-80/100 Submarine Applications," Military Specification MIL-S-1688A, Naval Sea Systems Command, Arlington, VA, 1990.
- M.J. Kleinosky, C.L. Trybus, D.L. Winterscheidt, and D.W. Yuan: *Advanced HY-80 Castings Heat Treatment Analysis*, NCEMT TR No. 00-36, Concurrent Technologies Corporation, Johnstown, PA, 2000.
- E.J. Czyryca: *Development of Low-Carbon, Copper-Strengthened HSLA Steel Plate for Naval Ship Construction*, DTRC-SME-90/21, David Taylor Research Center, Carderock, MD, 1990.
- R.K. Churchill, J.H. Devletian, and D. Singh: *High Yield Strength Cast Steel with Improved Weldability*, National Shipbuilding Research Program, NSRP No. 0326, Advanced Technology Institute, North Charleston, SC, 1991.
- Anon.: "Steel Castings, Alloy, High Yield Strength (HY-80 and HY-100)," Military Specification MIL-S-23008D (SH), Naval Sea Systems Command, Arlington, VA, 1990.
- K. Kannan, P.J. Konkol, J.R. Martinez, K. Ray, B.P. Tipton, and J.J. Valencia: *Evaluation of Candidate Casting Compositions (Interim Report): Enhanced Processing of High Strength Steel Castings and Forgings for Naval Components*, NCEMT TR No. 99-47, Concurrent Technologies Corporation, Johnstown, PA, 1999.

7. M.P. Seah, P.J. Spencer, and E.D. Hondros: *Met. Sci.*, 1979, vol. 13 (5), pp. 307-314.
8. W.G. Wilson, L.J. Heaslip, and I.D. Sommerville: *J. Met.*, 1985, vol. 37 (9), pp. 36-41.
9. C.I. Garcia, G.A. Ratz, M.G. Burke, and A.J. DeArdo: *J. Met.*, 1985, vol. 37 (9), pp. 22-28.
10. K. Kannan, K. Ray, J.R. Martinez, and P. J. Konkol: *Int. Symp. Steel for Fabricated Structures*, R. Asfahani and R. Bodnar, eds., ASM International, Materials Park, OH, 1999.
11. P.J. Konkol: Lenape Forge, West Chester, PA, private communication, 1998.
12. Anon.: "Standard Test Methods for Tension Testing of Metallic Materials," ASTM E8-98, ASTM, West Conshohocken, PA, 1998.
13. Anon.: "Standard Test Methods for Notched Bar Impact Testing of Metallic Materials," ASTM E23-96, ASTM, West Conshohocken, PA, 1996.
14. Anon.: "Standard Test Method for Dynamic Tear Testing of Metallic Materials," ASTM E604-83, ASTM, West Conshohocken, PA, 1994.
15. Anon.: "Oblique Y-Groove Test," AWS B4.0-95, American Welding Society, Miami, FL, 1995.
16. C.A. Papesch and J.J. Valencia: *Thermophysical Properties Determination of HSLA Steels*, NCEMT Laboratory Report TR No. 98-07, Concurrent Technologies Corporation, Johnstown, PA, 1999.
17. R.W. Fonda, J. Feng, and G. Spanos: "High Strength Steel Castings and Forgings for Naval Applications," *TMS 1999 Fall Meeting*, Cincinnati, OH, 1999.
18. S. Bechet and K. Rohrig: *Weldable High Strength Steel Cast Steel*, Climax Molybdenum Company Report, Greenwich, CT, 1982.
19. N.H. Croft, A.R. Entwisle, and G.J. Davies: *Advances in Physical Metallurgy and Applications of Steels*, The Metals Society, London, 1982, pp. 286-95.
20. Anon.: "Steel-Bars, Forgings, Bearing, Chain, Springs," ASTM Standard A 255, ASTM, West Conshohocken, PA, 2000, pp. 43-63.
21. D.W. Yuan, P.J. Konkol, K. Ray, B.P. Tipton, and J.J. Valencia: *Evaluation of Alternate High Strength Steel Forgings: Enhanced Processing of High Strength Steel castings and Forgings for the Naval Components*, NCEMT Report TR No. 99-32, Concurrent Technologies, Johnstown, PA, 1999.
22. G. Krauss: *Steels: Heat Treatment and Processing Principles*, ASM International, Materials Park, OH, 1990, p. 147.